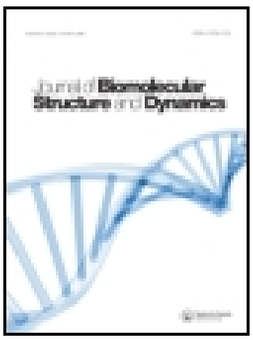

Taylor & Francis
Taylor & Francis Group

Journal of Biomolecular Structure and Dynamics

ISSN: (Print) (Online) Journal homepage: https://www.tandfonline.com/loi/tbsd20

Exploring 3-hydroxyflavone scaffolds as mushroom tyrosinase inhibitors: synthesis, X-ray crystallography, antimicrobial, fluorescence behaviour, structure-activity relationship and molecular modelling studies

Jamshaid Ashraf , Ehsan Ullah Mughal , Amina Sadiq , Maryam Bibi , Nafeesa Naeem , Anser Ali , Anam Massadaq , Nighat Fatima , Asif Javid , Muhammad Naveed Zafar , Bilal Ahmad Khan , Muhammad Faizan Nazar , Amara Mumtaz , Muhammad Nawaz Tahir & Masoud Mirzaei

To cite this article: Jamshaid Ashraf , Ehsan Ullah Mughal , Amina Sadiq , Maryam Bibi , Nafeesa Naeem , Anser Ali , Anam Massadaq , Nighat Fatima , Asif Javid , Muhammad Naveed Zafar , Bilal Ahmad Khan , Muhammad Faizan Nazar , Amara Mumtaz , Muhammad Nawaz Tahir & Masoud Mirzaei (2020): Exploring 3-hydroxyflavone scaffolds as mushroom tyrosinase inhibitors: synthesis, X-ray crystallography, antimicrobial, fluorescence behaviour, structure-activity relationship and molecular modelling studies, Journal of Biomolecular Structure and Dynamics, DOI: 10.1080/07391102.2020.1805364

To link to this article: https://doi.org/10.1080/07391102.2020.1805364

JOURNAL OF BIOMOLECULAR STRUCTURE AND DYNAMICS
https://doi.org/10.1080/07391102.2020.1805364

Exploring 3-hydroxyflavone scaffolds as mushroom tyrosinase inhibitors: synthesis, X-ray crystallography, antimicrobial, fluorescence behaviour, structure-activity relationship and molecular modelling studies

Jamshaid Ashraf[a], Ehsan Ullah Mughal[a], Amina Sadiq[b], Maryam Bibi[a], Nafeesa Naeem[a], Anser Ali[c], Anam Massadaq[c], Nighat Fatima[d], Asif Javid[a], Muhammad Naveed Zafar[e], Bilal Ahmad Khan[f], Muhammad Faizan Nazar[a], Amara Mumtaz[g], Muhammad Nawaz Tahir[h] and Masoud Mirzaei[i]

[a]Department of Chemistry, University of Gujrat, Gujrat, Pakistan; [b]Department of Chemistry, Govt. College Women University, Sialkot, Pakistan; [c]Department of Zoology, Mirpur University of Science and Technology, Mirpur, Pakistan; [d]Department of Pharmacy, COMSATS University Islamabad, Abbotabad, Pakistan; [e]Department of Chemistry, Quaid-i-Azam University, Islamabad, Pakistan; [f]Department of Chemistry, University of Azad Jammu and Kashmir, Muzaffarabad, Pakistan; [g]Department of Chemistry, COMSATS University Islamabad, Abbottabad, Pakistan; [h]Department of Physics, University of Sargodha, Sargodha, Pakistan; [i]Department of Chemistry, Faculty of Science, Ferdowsi University of Mashhad, Mashhad, Iran

Communicated by Ramaswamy H. Sarma

ABSTRACT

To explore new scaffolds as tyrosinase enzyme inhibitors remain an interesting goal in the drug discovery and development. In due course and our approach to synthesize bioactive compounds, a series of varyingly substituted 3-hydroxyflavone derivatives (**1-23**) were synthesized in one-pot reaction and screened for *in vitro* against mushroom tyrosinase enzyme. The structures of newly synthesized compounds were unambiguously corroborated by usual spectroscopic techniques (FTIR, UV-Vis, ^{1}H-, ^{13}C-NMR) and mass spectrometry (EI-MS). The structure of compound **15** was also characterized by X-ray diffraction analysis. Furthermore, the synthesized compounds (**1-23**) were evaluated for their antimicrobial potential. Biological studies exhibit pretty good activity against most of the bacterial-fungal strains and their activity is comparable to those of commercially available antibiotics *i.e.* Cefixime and Clotrimazole. Amongst the series, the compounds **2, 4, 5, 6, 7, 10, 11, 14** and **22** exhibited excellent inhibitory activity against tyrosinase, even better than standard compound. Remarkably, the compound **2** (IC_{50} = 0.280 ± 0.010 μg/ml) was found almost sixfold and derivative **5** (IC_{50} = 0.230 ± 0.020 μg/ml) about sevenfold more active as compared to standard Kojic acid (IC_{50} =1.79 ± 0.6 μg/ml). Moreover, these synthetic compounds (**1-23**) displayed good to moderate activities against tested bacterial and fungal strains. Their emission behavior was also investigated in order to know their potential as fluorescent probes. The molecular modelling simulations were also performed to explore their binding interactions with active sites of the tyrosinase enzyme. Limited structure-activity relationship was established to design and develop new tyrosinase inhibitors by employing 2-arylchromone as a structural core in the future.

Abbreviations: AFO: Algar-Flynn-Oyamada; Ala: Alanine; Asn: Asparagine; CA: *Candida albicans*; CP: *Candida parapsilosis*; DMSO: Dimethyl sulfoxide; E.coli: *Escherichia coli*; EI-MS: Electron impact mass spectrometry; FTIR: Fourier transformed infrared; Glu: Glutamic acid; His: Histidine; H_2O_2: Hydrogen peroxide; MMFF: Merck molecular force field; NMR: Nuclear magnetic resonance; PA: *Pseudomonas agaricus*; Phe: Phenylalanine; PDB: Protein data bank; SA: *Staphylococcus aureus*; TLC: Thin-layer chromatography; UV-Vis: Ultraviolet-visible spectroscopy; XRD: X-ray diffraction

ARTICLE HISTORY
Received 28 June 2020
Accepted 30 July 2020

KEYWORDS
3-hydroxyflavones; Algar-Flynn-Oyamada reaction; antibacterial; antifungal; tyrosinase enzyme inhibition; molecular docking studies

Introduction

Flavonoids belong to a class of naturally occurring polyphenolic compounds which are widely distributed in the vascular plant kingdom as secondary metabolites (Benavente-García et al., 1997; Farhadi et al., 2019; Hollman & Katan, 1999; Kumar & Pandey, 2013; Middleton, 1996; Seleem et al., 2017; Tschesche et al., 1979). Generally, they are recognized as the compounds possessing the C_6-C_3-C_6 carbon framework or more specifically a phenylbenzopyran skeleton, as core structure (Figure 1) (Aherne & O'Brien, 2002; Lopez-Lazaro, 2002; Tsao, 2010).

3-Hydroxyflavones or simply flavonols (Figure 1), also known as 3-hydroxy-2-phenyl-4*H*-1-benzopyran-4-ones, are the sub-category of the family of flavonoids that are ubiquitously found in the plants, fruits, and vegetables, etc. (Strack

CONTACT Ehsan Ullah Mughal ehsan.ullah@uog.edu.pk Department of Chemistry, University of Gujrat, Gujrat, 50700, Pakistan; Anser Ali anser.zoology@must.edu.pk Department of Zoology, Mirpur University of Science and Technology, Mirpur, 10250, AJK, Pakistan; Masoud Mirzaei mirzaeesh@um.ac.ir Department of Chemistry, Faculty of Science, Ferdowsi University of Mashhad, Mashhad, Iran.

Supplemental data for this article can be accessed online at https://doi.org/10.1080/07391102.2020.1805364.

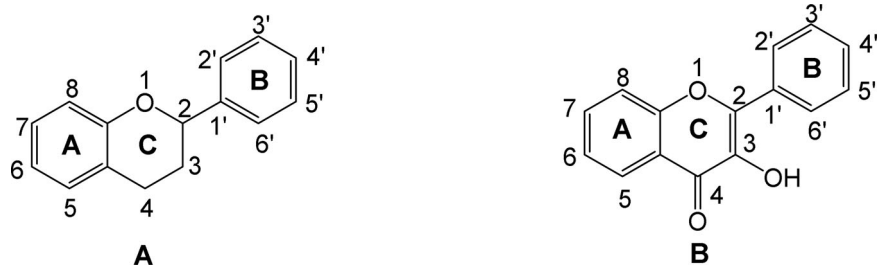

Figure 1. General structure of flavonoids (**A**) and 3-Hydroxyflavone (Flavonol) (**B**).

et al., 1994). Over the past decades, they have attained increasing attention on account of their immense biological activities and incredible health benefits (Alluis et al., 2000; Walle et al., 2003; Yoshida et al., 2009). For example, they are effective against cardiovascular diseases, inflammation (García-Lafuente et al., 2009), rheumatoid arthritis, diabetes, and asthma (Haslam, 1998; Rao et al., 2016). Recently, researchers have reported a number of significant pharmacological activities of these compounds (Cody et al., 1986; Hussin et al., 2009; Manthey et al., 2001; Ren et al., 2003; Rice-Evans et al., 1995). Additionally, they have been a subject of interest because of their ability to display a wide range of enzyme-modulatory properties against various enzymes (Agullo et al., 1997; Akiyama et al., 1987; Cushman et al., 1991; Ferriola et al., 1989; Gamet-Payrastre et al., 1999; Linassier et al., 1990; Liu et al., 2013; Mughal et al., 2019). Both natural and synthetic flavones have been shown to exhibit substantial biological activities including antimicrobial and enzymes inhibition (Verma & Pratap, 2010).

Tyrosinase inhibitors have attracted the attention of medicinal chemists because of their ability to inhibit the synthesis of melanin pigment (Chen & Kubo, 2002; Maeda & Fukuda, 1996). Their potential to decrease pigmentation gives them amazing applications in various fields, including the food industry (Tsuji-Naito et al., 2007), cosmetics (Nihei & Kubo, 2003) and medicines (Maeda & Yoshizaki, 1991). Melanin is a protein that has great importance for skin and hair color. It also possesses photo screening effects, provides skin photoprotection, and prevents skin injury. Despite its advantages, pigmentations can cause skin problems such as freckles, age spots, and melanoma. Therefore, control of melanin synthesis could be an effective strategy to control pigmentation related disorders. Tyrosinase is known as a rate limiting or the key enzyme for melanin synthesis. It catalyzes the hydroxylation of L-tyrosine to 3,4-dihydroxyphenylalanine (L-DOPA) and L-DOPA to dopaquinones (Cooksey et al., 1997) which cause abnormal melanin accumulation under unregulated conditions (Fairhead & Thöny-Meyer, 2012; Hearing & Jiménez, 1989). Thus, tyrosinase inhibition is the simplest and promising approach and tyrosinase inhibitors can be used for the prevention of conditions related to the hyperpigmentation of the skin, such as melasma and age spots. In this context, a number of both natural and synthetic polyphenols including flavonoids, phenolic acids, stilbenes, and lignans have been reported as weak or potent tyrosinase inhibitors (Chang, 2009; Kim et al., 2006; Promden et al., 2018; Qin et al., 2015; Şöhretoğlu et al., 2018; Zolghadri et al., 2019). Among these polyphenolic compounds, some of the flavonoid derivatives such as flavonols are considered to be the potent inhibitors of tyrosinase. There is a significant correlation between the inhibitory potency of flavonols on mushroom tyrosinase and melanin synthesis in melanocytes (Promden et al., 2018).

In the past decade, many natural and synthetic tyrosinase inhibitors have been evaluated, with many reported to also possess intrinsic antibacterial activity. Further, the enzyme product melanin has been shown to compromise the activity of traditional antibiotics. Due to the antibiotic resistance crisis and the slow development of new antibiotics, tyrosinase inhibitors may have the potential for the development of novel antimicrobials or antibiotic adjuvants that enhance the activity of incumbent drugs (Yuan et al., 2020). Recently, tyrosinase inhibitors have been also evaluated for their antibacterial activity, and some of them exhibit better potency compared with current antibiotics (Xia et al., 2014). It has been found that bacterial melanin can protect bacteria from UV radiation thereby increasing cell viability in the long term (Geng et al., 2008). In addition to protecting bacteria from UV radiation, melanin also chelates metals, increasing bacterial survival under environmental stress (Garcia-Rivera & Casadevall, 2001; Nosanchuk & Casadevall, 2003). More importantly, melanin can neutralize antibiotics, increasing the inhibitory dose of antibiotics, and improving the viability of bacteria.

In searching for promising mushroom tyrosinase inhibitors, many flavonols derivatives have been isolated and evaluated for their inhibitory activity on mushroom tyrosinase from different natural sources. However, their isolation procedure is lengthy, time-consuming, expensive, and boring as well. Also, natural sources are insufficient to meet the requirement all over the world.

Thus, laboratory synthesis may be considered as a substitute to the natural sources, in addition, it may also provide these compounds with structural variety.

To the best of our knowledge, there is no much literature available on the synthetic flavonols as competitive mushroom tyrosinase inhibitors except few examples (Kim et al., 2006; Promden et al., 2018; Qin et al., 2015; Zolghadri et al., 2019). Furthermore, among the tyrosinase inhibitors, carbonyl-based compounds including aurones, chalcones, flavanones, and pyrazole derivatives have gained attention owing to their interaction with the hydrophobic protein pocket nearby the binuclear copper active site of tyrosinase (Qin et al., 2015).

Encouraged by the potential pharmacological applications of flavonols and promising tyrosinase inhibitory potential of

related structures, we have been motivated to design and synthesize these novel compounds as potent mushroom tyrosinase inhibitors, and by keeping in mind the enhanced resistance of pathogens against antibiotics, it's also necessary to find new structurally varied flavonol-based drugs as antibiotics. Moreover, it is also desirous to study the inhibitory effect of various substituents at different positions and analyse how these compounds bind with tyrosinase protein at a molecular level. The experimental results were also verified by molecular docking studies.

Materials and methods

All the chemicals were purchased from Merck (Germany) and Sigma-Aldrich (USA) and used as delivered. Melting points were measured on an Electrothermal melting point apparatus and are uncorrected. The IR spectra were recorded on a Bio-Rad spectrophotometer. NMR spectra were measured on a Bruker DRX 300 instrument (^{1}H, 500 MHz, ^{13}C, 125 MHz). Accurate mass measurements were carried out with the Fisons VG sector-field instrument (EI) and a FT-ICR mass spectrometer. The IR values are mentioned in $\bar{\upsilon}$ units and NMR chemical shift values were determined in ppm units. Absorption spectra were recorded in very dilute solutions prepared in different solvents such as Acetonitrile, Methanol, DMSO on the Jasco UV-VIS V-670 instrument by using QUARTZ cell. Fluorescence spectra were recorded using Shimadzu 8101AFT-IR. Bruker Smart APEX-II CCD diffractometer was used for single crystal XRD studies.

Experimental X-ray diffraction details

X-ray data were collected at 296 K on a Bruker Kappa APEX II CCD diffractometer equipped with a graphite monochromator and a sealed molybdenum tube ($\lambda = 0.71073$ Å). The raw data were converted to F^2 values with *SAINT* (Bruker, 2016) while multiple measurements of equivalent reflections provided the basis for an empirical absorption correction as well as a correction for any crystal deterioration during the data collection (*SADABS*; Bruker, 2016). The structure was solved by direct methods and refined by full-matrix, least − squares procedures using the *SHELXTL* program package (Bruker, 2016). Hydrogen atoms were included as riding contributions in idealized positions with isotropic displacement parameters tied to those of the attached atoms. Satisfactory hydrogen bond parameters were achieved with this model. The *PLATON* software (Spek, 2015) was used to calculate bond distances, bond angles, torsion angles, hydrogen bonds, and other geometric parameters. The Mercury 3.7 software (Macrae et al., 2006) was used to generate the figures and to perform other calculations (Bruker, 2016; Macrae et al., 2006; Spek, 2009, 2015). The crystal data and refinement of the given in Table S1.

General procedure for the synthesis of 3-hydroxyflavone derivatives (1-23)

A mixture of *o*-hydroxyacetophenone (1.2 mL, 10.0 mmol) in aqueous 30% sodium hydroxide solution was stirred in methanol (20.0 mL) for 30 min at ambient temperature followed by the addition of substituted benzaldehyde (10.0 mmol). This reaction mixture was allowed to stir for further 4.0 h at the same temperature. The progress of the reaction was monitored by comparative TLC. After the completion of the reaction (checked by TLC), 2′-Hydroxychalcone, formed *in situ*, was further oxidatively cyclized by adding 1.5 mL of 35% H_2O_2 to the same reaction mixture which was then allowed to stir for additional 1.0 h. Afterward, 10% aqueous HCl was added to the reaction mixture in order to neutralize it, and as a result flavonols (3-hydroxyflavones) were precipitated out. These precipitates were then filtered, washed with water and subsequently with cold ethanol. Residue obtained was collected, dried, and finally recrystallized by ethanol (Mughal et al., 2019).

Biological evaluation studies

Antifungal activity

Antifungal activities of all the synthesized compounds were determined by employing known "Well Diffusion Method". Two fungal strains were used one was *Candida parapsilosis* (CP) (ATCC#22019) and the second one was the *Candida albicans* (CA) (ATCC#9002). The standard drug used was Clotrimazole, 1.0 mg of the Clotrimazole taken in 1.0 mL of DMSO. In mm zone of inhibition was measured and this zone of inhibition was the antifungal potential. The amount of DMSO taken to prepare the sample was 1 mL and the 3.0 mg of the sample dissolved in this DMSO SDA plates were used to spread the sample. These are pre-prepared plates made up of Sabouraud dextrose agar. The spreading of the sample on SDA plates was assisted by using a sterile glass rod. The depth of the well prepared by using the sterile cork bore and it was 8 mm and all of these wells were at the appropriated distance from each other. Sample taken for analysis was 80 µL, samples along with standards were poured on their appropriate wells. 24–46 h were utilized and the prepared plates were incubated. The antifungal activity recorded in mm units and it was calculated by the measuring zone of inhibition (Mughal, Sadiq, et al., 2018).

Antibacterial activity

Antibacterial activity against different strains of bacteria was measured. The method used for measuring the antibacterial potential was the disc diffusion method (Mughal, Sadiq, et al., 2018). The bacterial strains used were *Escherichia coli* (ATCC#25922), *Pseudomonas aeruginosa* (ATCC#9721), and *Staphylococcus aureus* (ATCC#6538). The zone of inhibition was measured as the antibacterial potential of the synthesized compounds. Two controls were used one is positive Cefixime and the other is negative DMSO. Different samples of the compounds were prepared by dissolving 4 mg of the sample into 1 mL of the DMSO. The lawn created on nutrient agar plates by using bacterial strains having equivalent

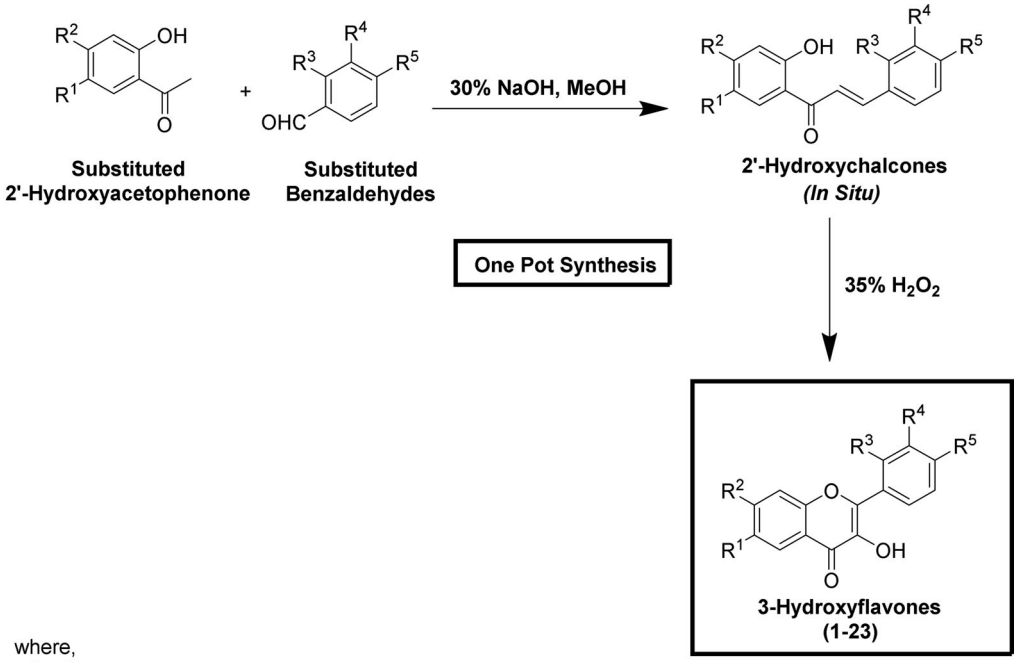

where,
R^1, R^2 = -H, -CH_3, -Br, -Cl
R^3, R^4, R^5 = -OCH_3,-CF_3, -NO_2, -Cl, -Br, -F, *etc.*

Compound No.	Structures	Compound No.	Structures
1	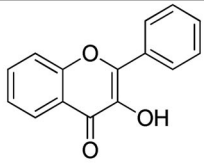	13	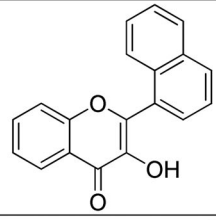
2	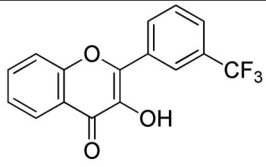	14	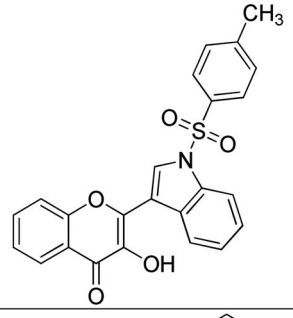
3	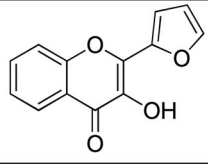	15	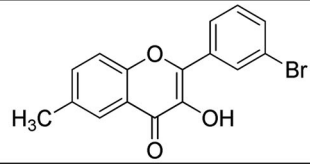

Scheme 1. Synthesis of varyingly substituted 3-hydroxyflavone derivatives (**1-23**).

turbidity that is attained by using 0.5% of McFarland solution. The depth of the well was 8 mm and they were all made at the appropriate distances from each other. The sample and the standard were poured into their appropriate wells. The amount of sample used was 80 µL in a well and along with the two control. At 37 °C the prepared plates were incubated for 24 h and zone of inhibition usually measured in mm and diameter of the zone of inhibition was expressed as the potential of samples against used bacterial strains.

Enzyme inhibition activity

Mushroom anti-tyrosinase assay. The mushroom tyrosinase enzyme was used to access *in vitro* anti-tyrosinase activity of the test compounds as described previously with some

4	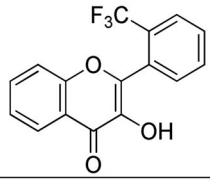	**16**	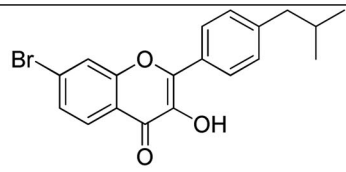
5	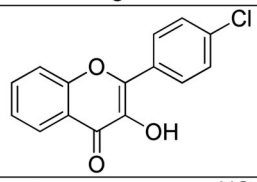	**17**	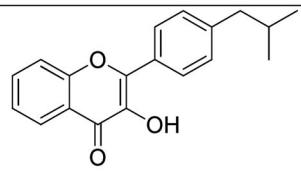
6	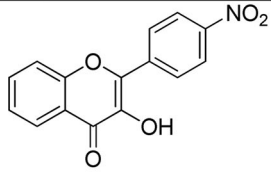	**18**	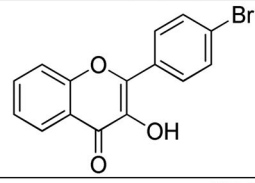
7	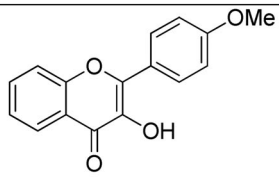	**19**	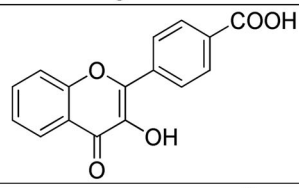
8	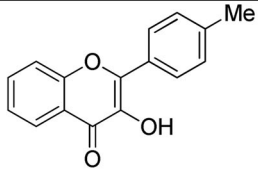	**20**	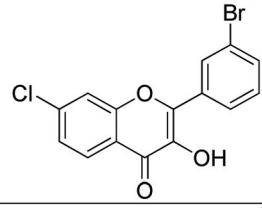
9	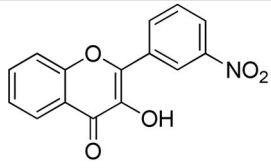	**21**	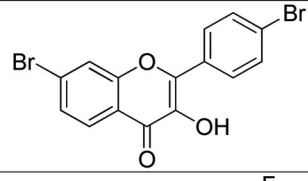
10	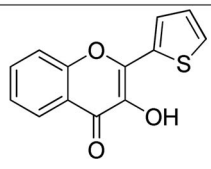	**22**	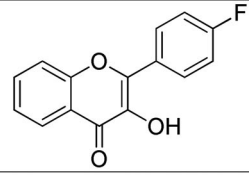
11	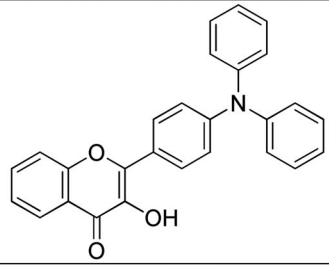	**23**	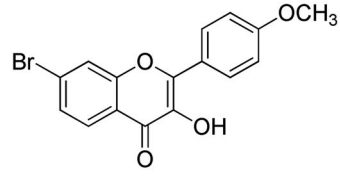
12	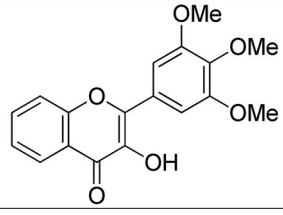		

Scheme 1. (Continued).

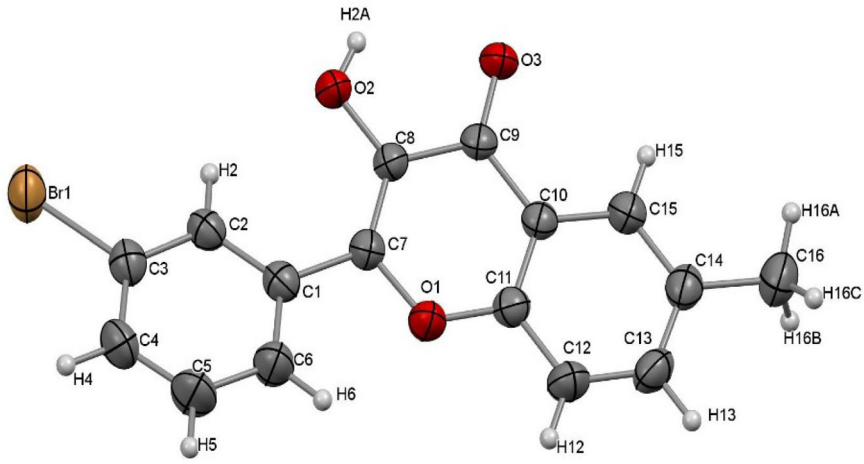

Figure 2. ORTEP diagram of the compound **15** showing 30% probability thermal ellipsoids and the atom-numbering scheme.

modifications (Ali et al., 2016; Seo et al., 2010). Briefly, 140 μL of phosphate buffer (20 mM, pH 6.8), 20 μL of mushroom tyrosinase (30 U/ml), and 20 μL of test compound were mixed in the wells of a 96-well plate. After 10 min incubation at room temperature, 20 μL (0.85 mM) of 3,4-dihydroxyphenylalanine (L-DOPA) was added. The plate was incubated at 25 °C for 20 min in dark. Later, the absorbance of dopachrome was monitored at 400 nm using a plate reader (Bio Tek ELX 808). Percentage inhibition was calculated by the following formula:

$$\text{Inhibition } (\%) = [(\text{B}--\text{a})/\text{B}] \times 100$$

where, A = absorbance of enzyme with the test compound and, B = absorbance of the enzyme without test compound. Later, the concentration of test compounds necessary to achieve 50% tyrosinase inhibition (IC_{50}) was determined by the data analysis and graphing software, Origin.

Molecular docking studies

In order to carry out the docking studies, various tools are available for the study of protein-ligand associations, Autodock 1.5.6 was applied for their automation capability (Ehsan U Mughal, Sadiq, et al., 2018). The crystal structure of *Agaricus bisporus* tyrosinase (PDB ID: 2Y9X) was obtained, from RCSB protein data bank (PDB), as a model. 3D grids of tropolone in the binding pocket of tyrosinase was estimated by using discovery studio 4.0. The protein structure was optimized and side-chain hydrogens were added. Total Koll man charges (−820.404) were added to the tyrosinase targeted biological molecule.

Results and discussion

Chemistry

3-Hydroxyflavones (**1-23**) were synthesized starting from 2′-hydroxyacetophenone and differently substituted benzaldehydes in one-pot synthesis through Algar-Flynn-Oyamada (AFO) reaction (Scheme 1). 2′-Hydroxyacetophenone underwent Claisen-Schmidt condensation with various benzaldehydes in methanolic-sodium hydroxide solution to produce 2′-hydroxychalcones as key intermediates. 2′-Hydroxychalcones, generated *in situ*, were then cyclized into flavonols (**1-23**) through oxidative cyclization using 35% hydrogen peroxide (H_2O_2) under basic medium and same solvent. All the synthesized target compounds (**1-23**) were purified by recrystallization in ethanol and obtained in moderate to excellent yields, and are soluble in common solvents for instance acetone, acetonitrile, methanol, chloroform, and DMSO, etc. Subsequently, all the newly synthesized compounds were characterized by FTIR, UV-Vis, and NMR spectroscopic techniques. In addition, their accurate molecular masses were determined by electron ionization (EI) mass spectrometry. All the spectral data unequivocally confirm the structures of the newly synthesized molecules.

Furthermore, the single-crystal for the compound **15** was grown through recrystallization in ethanol, and its molecular structure was determined by single-crystal X-ray analysis (Altaf et al., 2017; Bruker, 2016; Lal et al., 2016; Macrae et al., 2006; Saleem et al., 2018; Spek, 2009, 2015) and is displayed in Figure 2 and other details are given in supporting information.

The spectroscopic data of all the newly synthesized compounds **2, 4, 11, 13, 14, 15,** and **20** are given below. However, the spectral data of the remaining compounds are given in the literature (Bansal & Kaur, 2015; Ehsan et al., 2016; Golub et al., 2011; Gunduz et al., 2012; Gupta et al., 2012, 2014; Höfener et al., 2013; Kaur et al., 2017; Khanna et al., 2015; Klymchenko et al., 2001; Mughal, Javid, et al., 2018; Mughal et al., 2019; Nhu et al., 2015; Singh et al., 2017; You et al., 2020).

2-(3-(trifluoromethyl)phenyl)-3-hydroxy-4H-chromen-4-one (2)

Bright-yellow crystalline solid; Yield: 76%; m.p. 178–180 °C; R_f (Ethyl acetate: *n*-hexane 1:3) = 0.8; UV-Vis λ_{max} (Methanol) = 255, 370 nm; FTIR (cm^{-1}): 3096, 1607, 1483, 1318, 1209, 1111, 1085, 964; ^{1}H NMR (300 MHz, DMSO-d_6): δ 10.00 (bs, 1H, OH), 8.57 (s, 1H, Ar–H), 8.51 (d, 1H, *J* = 6.0 Hz, Ar–H), 8.14–8.10 (m, 1H, Ar–H), 7.89–7.80 (m, 4H, Ar–H), 7.52–7.46 (m, 1H, Ar–H);

^{13}C NMR (75 MHz, DMSO-d_6): δ 173.0, 154.8, 143.4, 140.1, 134.3, 132.7, 131.4, 130.2, 130.0, 129.4, 126.4, 125.2, 125.0, 124.5, 122.0, 118.8; accurate mass (EI-MS) of $[M]^{+\cdot}$: Calcd. for $C_{16}H_9F_3O_3$ 306.05037; found 306.05025.

2-(2-(trifluoromethyl)phenyl)-3-hydroxy-4H-chromen-4-one (4)

Dull-yellow solid; Yield: 70%; m.p. 187–189 °C; R_f (Ethyl acetate: *n*-hexane 1:3) = 0.6; UV-Vis λ_{max} (Methanol) = 273, 320 nm; FTIR (cm^{-1}): 3297, 1688, 1443, 1367, 1285, 1243, 1153, 1103, 1034, 844; ^{1}H NMR (300 MHz, DMSO-d_6): δ 9.98 (bs, 1H, OH), 8.70–8.50 (m, 2H, Ar–H), 7.85–7.65 (m, 4H, Ar–H), 7.60–7.49 (m, 2H, Ar–H); ^{13}C NMR (75 MHz, DMSO-d_6): δ 173.1, 154.7, 143.6, 140.2, 135.0, 132.8, 131.1, 131.5, 130.1, 129.6, 127.0, 125.5, 125.1, 124.4, 122.1, 118.7; accurate mass (EI-MS) of $[M]^{+\cdot}$: Calcd. for $C_{16}H_9F_3O_3$ 306.05037; found 306.05021.

2-(4-(diphenylamino) phenyl)-3-hydroxy-4H-chromen-4-one (11)

Mustard-yellow crystalline solid; Yield: 90%; m.p. 188–190 °C; R_f (Ethyl acetate: *n*-hexane 1:3) = 0.7; UV-Vis λ_{max} (Methanol) = 293, 393 nm; FTIR (cm^{-1}): 3221, 1686, 1481, 1410, 1329, 1154, 1134, 824; ^{1}H NMR (300 MHz, $CDCl_3$): δ 9.74 (s, 1H, OH), 7.63–7.58 (m, 2H, Ar–H), 7.30–7.24 (m, 6H, Ar–H), 7.12–7.07 (m, 8H, Ar–H), 6.96 (d, J = 9.0 Hz, 2H, Ar–H), ^{13}C NMR (75 MHz, $CDCl_3$): δ 181.5, 153.4, 146.1, 131.4, 129.7, 129.3, 126.3, 126.2, 125.0, 118.3, the other carbons are isochronous; accurate mass (EI-MS) of $[M]^{+\cdot}$: Calcd. for $C_{27}H_{19}NO_3$ 405.13649; found 405.13640.

2-(naphthalen-1-yl)-3-hydroxy-4H-chromen-4-one (13)

Light-yellow solid; Yield: 80%; m.p. 177–179 °C; R_f (Ethyl acetate: *n*-hexane 1:3) = 0.8; UV-Vis λ_{max} (Methanol) = 251, 330 nm; FTIR (cm^{-1}): 3051, 1603, 1461, 1416, 1342, 1142, 670, 571; ^{1}H NMR (300 MHz, DMSO-d_6): δ 8.24–8.14 (m, 1H, Ar–H), 8.00 (dd, J = 9.0, 3.0 Hz, 1H, Ar–H), 7.89–7.80 (m, 3H, Ar–H), 7.68 (dd, J = 9.0, 3.0 Hz, 1H, Ar–H), 7.57 (ddd, J = 9.0, 6.0, 3.0 Hz, 1H, Ar–H), 7.52–7.48 (m, 2H, Ar–H), 7.45–7.38 (m, 2H, Ar–H); ^{13}C NMR (75 MHz, DMSO-d_6): δ 173.4, 168.0, 158.7, 154.2, 140.3, 136.1, 133.4, 130.5, 127.8, 127.0, 124.7, 118.2; accurate mass (EI-MS) of $[M]^{+\cdot}$: Calcd. for $C_{19}H_{12}O_3$ 288.07864; found 288.07870.

2-(1-tosyl-1H-indol-3-yl)-3-hydroxy-4H-chromen-4-one (14)

Dirty-yellow crystalline solid, Yield: 78%; m.p. 244–246 °C; R_f (Ethyl acetate: *n*-hexane 1:3) = 0.7; UV-Vis λ_{max} (Methanol) = 254, 297 nm; FTIR (cm^{-1}): 3356, 2190, 1656, 1447, 1394, 1161, 1130, 692; ^{1}H NMR (300 MHz, DMSO-d_6): δ 9.89 (s, 1H, OH), 8.45 (s, 1H, Ar–H), 8.26 (s, 1H, Ar–H), 8.12–7.95 (m, 2H, Ar–H), 7.74 (d, J = 9.0 Hz, 1H, Ar–H), 7.52 (d, J = 9.0 Hz, 2H, Ar–H), 7.31–7.18 (m, 1H, Ar–H), 7.14 (d, J = 9.0 Hz, 2H, Ar–H), 6.97–6.87 (m, 1H, Ar–H), 6.53 (d J = 9.0 Hz, 1H, Ar–H), 6.36 (t, J = 9.0 Hz, 1H, Ar–H), 2.28 (s, 3H, CH_3); ^{13}C NMR (75 MHz, DMSO-d_6): δ 171.2, 167.7, 154.1, 150.5, 145.4, 141.0, 139.5, 138.5, 132.2, 131.8, 130.3, 128.6, 125.9, 124.6, 123.7, 121.1, 120.9, 120.4, 118.4, 117.1, 115.6, 114.2, 113.1, 21.3; accurate mass (EI-MS) of $[M]^{+\cdot}$: Calcd. for $C_{24}H_{17}NO_5S$ 431.08274; found 431.08265.

2-(3-bromophenyl)-3-hydroxy-6-methyl-4H-chromen-4-one (15)

Mustard-yellow crystalline solid; Yield: 87%; m.p. 179–181 °C; R_f (Ethyl acetate: *n*-hexane 1:3) = 0.6; UV-Vis λ_{max} (Acetonitrile) = 241, 332 nm; FTIR (cm^{-1}): 3228, 2115, 1604, 1568, 1554, 1487, 1463, 1282, 1137, 1093; ^{1}H NMR (500 MHz, CD_2Cl_2): δ 9.67 (s, 1H, OH), 7.95 (s, 1H, Ar–H), 7.86 (s, 1H, Ar–H), 7.78 (d, J = 10.0 Hz, 1H, Ar–H), 7.59 (d, J = 10.0 Hz, 1H, Ar–H), 7.40–7.37 (m, 1H, Ar–H), 7.27–7.25 (m, 1H, Ar–H), 7.10–7.07 (m, 1H, Ar–H); ^{13}C NMR (125 MHz, DMSO-d_6): δ 173.4, 153.4, 143.5, 140.0, 135.7, 134.6, 134.1, 132.8, 131.1, 130.3, 126.8, 124.3, 122.3, 121.4, 118.8, 20.8; accurate mass (EI-MS) of $[M]^{+\cdot}$: Calcd. for $C_{16}H_{11}BrO_3$ 329.98915; found 329.98902.

2-(3-bromophenyl)-3-hydroxy-6-chloro-4H-chromen-4-one (20)

Dark-yellow solid, Yield: 80%; m.p. 189–191 °C; R_f (Ethyl acetate: *n*-hexane 1:3) = 0.8; UV-Vis λ_{max} (Acetonitrile) = 244, 334 nm; FTIR (cm^{-1}): 3246, 3055, 2902, 1625, 1606, 1567, 1387, 1259, 1210, 1139; ^{1}H NMR (500 MHz, DMSO-d_6): δ 9.87 (s, 1H, OH), 8.40 (s, 1H, Ar–H), 8.22 (d, J = 5.0 Hz, 1H, Ar–H), 7.90 (s, 1H, Ar–H), 7.71 (d, J = 10.0 Hz, 2H, Ar–H), 7.64, (dd, J = 10.0, 5.0 Hz, 1H, Ar–H), 7.54 (t, J = 10.0 Hz, 1H, Ar–H), 2.45 (s, 3H, CH_3); ^{13}C NMR (125 MHz, CD_2Cl_2): δ 172.5, 159.0, 139.0, 137.4, 135.5, 133.6, 132.2, 131.7, 130.4, 129.8, 128.3, 127.8, 126.5, 121.4, 120.1; accurate mass (EI-MS) of $[M]^{+\cdot}$: Calcd. for $C_{15}H_8BrClO_3$ 349.93453; found 349.93461.

UV-visible spectroscopic analysis

The UV-visible analysis was carried out mostly in methanol. In general, flavonols show two maxima in the range of 250–285 nm and 320–385 nm corresponding to benzoyl ring (Ring A) and cinnamoyl ring (Ring B) respectively. The UV-vis spectra of some of all the newly synthesized compounds have been displayed in supporting information (SI).

Fluorescence behavior

Emission wavelengths were recorded for the synthesized 3-hydroxyflavone derivatives (**1-23**) mostly in methanol and acetonitrile solvents. The results are listed in Table 1.

3-Hydroxyflavone derivatives have great potential as fluorescence probes for bio-labelling in aqueous medium (Ehsan et al., 2016; Gupta et al., 2012, 2014; Mughal, Javid, et al., 2018; Singh et al., 2017). This property comes from its well-separated dual emission bands in fluorescence spectra, originated from normal (N*) and photo tautomer forms (T*) of an excited state intramolecular proton transfer reaction (Figure 3). The fluorescent behavior of these compounds has been studied in various organic solvents using emission spectroscopy, performed at room temperature. The synthesized

Table 1. Fluorescence analysis results.

Compound Number	Excitation Wavelength Values (nm)	Emission Wavelength Values (nm) (Solvent)
1	386	403, 531 (Methanol)
2	380	402, 540 (Methanol)
3	395	417, 533 (Methanol)
4	330	404, 546 (Methanol)
5	363	400, 538 (Methanol)
6	365	402, 537 (Methanol)
7	373	409, 529 (Methanol)
8	373	473, 602 (Methanol)
9	355	412, 532 (Methanol)
10	370	390, 698 (Methanol)
11	403	426, 541 (Methanol)
12	371	441, 591 (Methanol)
13	340	481 (Methanol)
14	307	423, 582 (Methanol)
15	342	411, 546 (Methanol)
16	335	470, 537 (Methanol)
17	362	530 (Acetonitrile)
18	358	404, 536 (Acetonitrile)
19	372	402, 537 (Acetonitrile)
20	344	428, 535 (Acetonitrile)
21	336	549 (Acetonitrile)
22	320	528 (Acetonitrile)
23	380	541 (Acetonitrile)

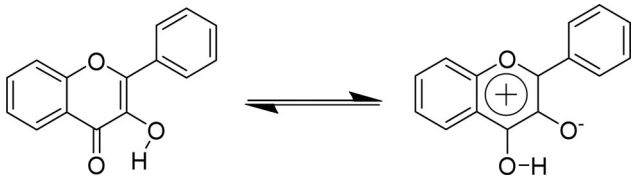

Figure 3. Conversion of simple flavonol (**1**) from normal electronic state to excited electronic state.

compounds, when irradiated with ultraviolet radiation, were observed to have fluorescence properties in the blue portion of the visible spectrum. In comparison, emission intensities showed that the alkyl groups have a surprising effect on the emission strength of 3-hydroxyflavone derivatives. The alkyl substitution at the aryl group (ring B) can be expected to have some effect on the physico-chemical properties due to its electron-donating nature and if we replaced the 2-phenyl group of 3-hydroxyflavone with any heterocyclic compound having extended conjugation, the product exhibited better fluorescence properties than 3-hydroxyflavone, for example, the compound **10** (Table 1). From the emission spectra of the reported compounds, it can be concluded that the introduction of electron-donating groups at ring B significantly affects the emission intensity without causing any major blue or red-shift in the emission wavelength, and electron-withdrawing groups offer reverse effect. The emission spectra of all the compounds (**1-23**) have been shown in SI.

Antimicrobial evaluation

The growing resistance of microorganisms to standard antibiotics encourages the search for novel antimicrobial agents. In this context, the antibacterial activities of all the synthesized compounds (**1-23**) were tested against a panel of one Gram-positive Bacterium *Staphylococcus aureus* (SA, ATCC#6538) and two Gram-negative Bacteria *Escherichia coli* (E-coli, ATCC# 25922) and *Pseudomonas aeruginosa* (PA, ATCC#9721) using conventional agar well diffusion method. Similarly, anti-fungal activities of the same compounds were evaluated against two fungi *Candida albicans* (CA, ATCC#9002) and *Candida parapsilosis* (CP, ATCC# 22019) using the previously mentioned method. Cefixime and Clotrimazole were used as standard drugs. The results were recorded for each tested compound as the average diameter of inhibition zones (IZ) of bacterial or fungal growth around the discs in mm. The antibacterial and antifungal results are displayed in Tables 2 and 3 respectively.

Antibacterial activity

The antibacterial assay revealed that these compounds are relatively more active against *P. aeruginosa* and *E. coli* than *S. aureus*. Noteworthy, simple flavonol **1** is least active amongst the series. However, by introducing various substituents on flavonol scaffold led to an increased antibacterial activity. This finding most probably resulted from the high hydrophobicity of such compounds. It is obvious that the compounds **4, 14, 19, 20, 21, 22** and **23**, which contain mostly electron-withdrawing groups, exhibited the highest activity against both *P. aeruginosa* and *E.coli*, whereas the compounds **3, 15, 17** and **18** showed the highest activity against *P. aeruginosa* (Table 2). Their activities were found to be comparable with that of standard drug tested (Cefixime). In comparison, the envisioned derivatives are more active against P. *aeruginosa* than *E. coli*. Moreover, the other compounds among the series manifested moderate to good activities against the tested bacterial strains.

Antifungal activity

The lesser number of available harmless antifungal agents is the driving force to search for new candidates. The promising antibacterial activity of the tested compounds has encouraged us to test these compounds against two different pathogenic fungi. In general, all the compounds screened exhibited moderate to good activity against both *C. albicans* and *C. parapsilosis* fungi (Table 3). However, these derivatives were found comparatively more active against *C. parapsilosis* than *C. albicans*. For instance, amongst the series,

Table 2. Potential of 3-hydroxyflavone derivatives (**1-23**) against bacterial strains.

	Zones of Inhibition (mm)		
Compound Number	*PA*	*SA*	*E-COLI*
1	7.2 ± 0.2	NA*	9.6 ± 0.6
2	14.2 ± 0.7	16.6 ± 0.7	14.6 ± 0.7
3	20.3 ± 0.5	23.5 ± 0.4	12.7 ± 0.6
4	22.2 ± 0.5	19.4 ± 0.6	20.5 ± 0.2
5	16.6 ± 0.6	16.6 ± 0.3	16.8 ± 0.6
6	14.2 ± 0.6	18.7 ± 0.3	14.7 ± 0.8
7	15.4 ± 0.6	NA	14.5 ± 0.7
8	14.1 ± 0.5	NA	14.7 ± 0.8
9	17.2 ± 0.4	NA	16.7 ± 0.4
10	16.2 ± 0.3	NA	20.5 ± 0.2
11	18.7 ± 0.2	20.7 ± 0.	18.5 ± 0.7
12	14.1 ± 0.5	NA	16.5 ± 0.6
13	18.1 ± 0.2	11.1 ± 0.1	19.1 ± 0.4
14	25.1 ± 0.4	NA	26.1 ± 0.3
15	24.1 ± 0.4	19.2 ± 0.2	24.5 ± 0.4
16	9.4 ± 0.2	NA	19.1 ± 0.3
17	21.1 ± 0.2	NA	19 ± 0.1
18	24.2 ± 0.3	20.2 ± 0.3	18 ± 0.3
19	25.2 ± 0.3	23.2 ± 0.1	20 ± 0.2
20	19.2 ± 0.1	NA	22.5 ± 0.5
21	25.4 ± 0.6	NA	26.5 ± 0.3
22	25.2 ± 0.6	21.0 ± 0.5	27.5 ± 0.6
23	NA	NA	24.1 ± 0.4
DMSO	NA	NA	NA
Cefixime (1 mg/ml)	28.7 ± 0.3	27.5 ± 0.7	30.5 ± 0.3

*NA = No Activity.

Table 3. Potential of 3-hydroxyflavone derivatives (**1-23**) against fungal strains.

	Zones of Inhibition (mm)	
Compound Number	*CA*	*CP*
1	14.5 ± 0.5	11.8 ± 0.5
2	15.7 ± 0.9	NA*
3	14.6 ± 0.6	19.7 ± 0.6
4	13.6 ± 0.6	14.6 ± 0.4
5	NA	13.6 ± 0.5
6	NA	NA
7	NA	19.6 ± 0.7
8	NA	NA
9	NA	NA
10	17.5 ± 0.9	16.5 ± 0.4
11	19.6 ± 0.3	14.6 ± 0.8
12	16.5 ± 0.2	21.5 ± 0.3
13	23.5 ± 0.1	20.5 ± 0.2
14	20.4 ± 0.1	22.7 ± 0.2
15	14.2 ± 0.2	21.1 ± 0.4
16	18.5 ± 0.3	19.1 ± 0.6
17	15.3 ± 0.3	17.3 ± 0.5
18	9.3 ± 0.3	20.2 ± 0.4
19	20.3 ± 0.0	21.2 ± 0.6
20	19.4 ± 0.3	21.5 ± 0.2
21	10.2 ± 0.2	NA
22	18.3 ± 0.3	20.3 ± 0.2
23	20.3 ± 0.5	21.6 ± 0.2
DMSO	NA	NA
Clotrimazole (1 mg/ml)	28.9 ± 0.8	25.6 ± 0.6

*NA = No Activity.

the compounds **3, 7, 12, 13, 14, 15, 16, 18, 19, 20, 22,** and **23** exhibited the highest activity against *C. parapsilosis*. Although with respect to the standard drugs, all the evaluated compounds were found to show moderate activity, so the result of all preliminary study indicated that the flavonol moiety containing compounds represent a new class of pharmacophore for broad-spectrum antibacterial and antifungal activity.

Table 4. Tyrosinase inhibitory efficacy of synthesized derivatives (**1-23**).

Compounds	Mushroom Tyrosinase Inhibition IC_{50}±SEM[a] (μg/ml)
1	4.268 ± 0.182
2	0.280 ± 0.010
3	n.d*
4	0.30 ± 0.0
5	0.230 ± 0.020
6	0.284 ± 0.018
7	1.787 ± 0.445
8	14.171 ± 0.855
9	2.564 ± 0.251
10	0.347 ± 0.078
11	0.327 ± 0.041
12	n.d*
13	2.90 ± 0.032
14	0.370 ± 0.025
15	13.912 ± 3.339
16	19.595 ± 0.515
17	4.844 ± 0.347
18	4.437 ± 0.032
19	35.189 ± 2.384
20	5.783 ± 0.642
21	7.226 ± 0.589
22	0.799 ± 0.008
23	2.236 ± 0.008
Kojic Acid[b]	1.79 ± 0.6

[a]IC_{50} values (mean ± standard error of the mean);
[b]Standard inhibitor for mushroom tyrosinase;
*n.d = not determined.

Mushroom tyrosinase inhibition assay. In continuation of our efforts on enzyme inhibition activity (Mughal, Javid, et al., 2018; Mughal, Sadiq, et al., 2018; Mughal et al., 2019), 3-hydroxyflavones (**1–23**) were synthesized and evaluated, *in vitro*, for their anti-tyrosinase activity. Kojic acid (IC_{50} = 1.79 ± 0.6 μg/ml) was used as a reference compound. The IC_{50} values of tested compounds are summarized in Table 4, and these values are presented as the mean of three experiments. The obtained results revealed that most of the compounds displayed potent inhibition on mushroom tyrosinase enzyme with IC_{50} values ranging from 0.230 ± 0.020 μg/ml to 35.189 ± 2.384 μg/ml except the compounds **3** and **12** whose IC_{50} values were not determined (Table 4).

Structure-activity relationship of mushroom tyrosinase inhibitory activity

The general structure of the flavonol nucleus is comprised of a chromone moiety and an aryl ring (B) (Figure 1). All these structural features are playing a significant role in inhibitory activity, however, a little variation in the activity of these compounds is attributed to variability in the positions and nature of substituents on aryl ring (B) as well as the nature of ring B. Limited SAR studies was established purely on the basis of substitution pattern on the 3-hydroxyflavone scaffold (Figure 4). In this connection, compound **1** (IC_{50} = 4.268 ± 0.182 μg/ml) bearing no substituent displayed the least activity amongst the series. However, the substituted derivatives demonstrated very good inhibitory activities in comparison to flavonol **1** presenting that substitution on rings A & B increases the inhibitory potential of these compounds. Additionally, compounds **8, 15, 16,** and **19** were found to be less active against the envisioned enzyme. These findings reflect that highly hydrophilic (i-e –COOH) and

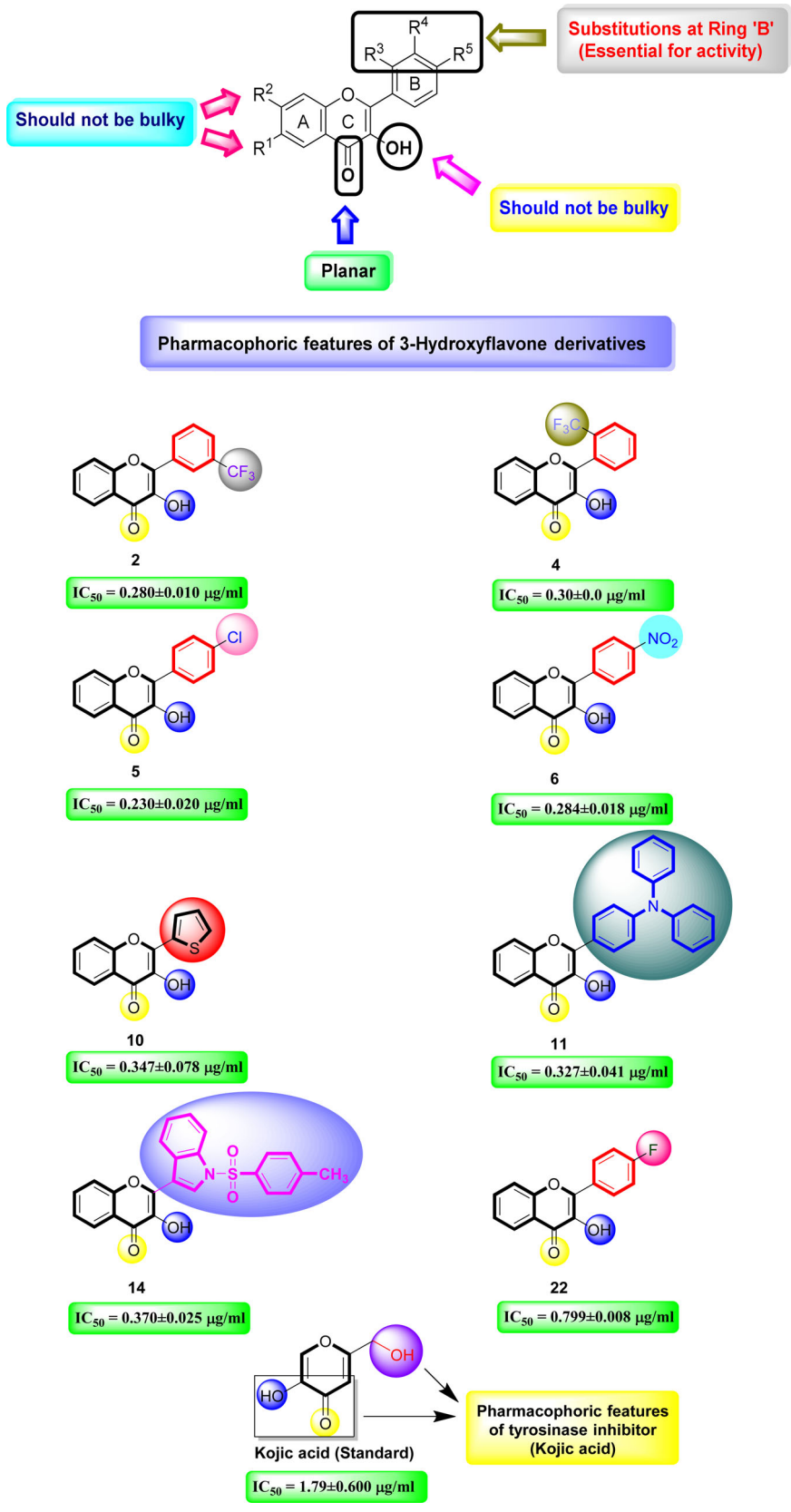

Figure 4. Pharmacophoric features of 3-hydroxyflavones and tyrosinase inhibitor, structure-activity relationship (SAR) of the most potent compounds.

hydrophobic (–CH_3 and *iso*-butyl) groups on both aryl rings (A & B) are accountable for their low activities because of their less interaction with the enzyme.

It is noteworthy that the derivatives **2, 4, 5, 6, 10, 11, 14,** and **22** demonstrated exceptional inhibitory activity against tyrosinase enzyme. All these compounds are even more active than the reference compound. Excitingly, the test compounds **2** (IC_{50} = 0.280 ± 0.010 µg/ml) and **5** (IC_{50} = 0.230 ± 0.020 µg/ml) were found to be the most active, among all the synthesized analogs, as compared to the

Table 5. Binding energies of selective modes against tyrosinase enzyme.

Compound No.	Lowest Binding Energy (Kcal mol^{-1})
1	−6.67
2	−7.98
3	−6.38
4	−7.42
5	−8.55
6	−8.47
7	−7.10
8	−7.27
9	−7.05
10	−7.05
11	−9.56
12	−6.63
13	−8.94
14	−8.59
15	−7.05
16	−7.30
17	−6.71
18	−6.55
19	−6.33
20	−7.10
21	−7.06
22	−6.31
23	−6.83
Standard (Tropolone)	−4.44

standard Kojic acid (IC_{50} =1.79 ± 0.6 μg/ml). The derivative **2** possesses a highly electron-withdrawing group (–CF_3) at *meta*- position on ring B. This indicates that the structure **2** nicely fits and strongly interacts with the active site of the envisioned enzyme. Interestingly, the analogous **4** (IC_{50} = 0.30 ± 0.0 μg/ml), having trifluoromethyl group –CF_3) at the *ortho*- position of ring B, was found comparatively less active than its *meta*-isomer **2,** but still more active than standard. Furthermore, the flavonol **5** bears electron-withdrawing group (–Cl) at 4′ -position on ring B. Probably, this group and its position are appropriate to agreeably interact with the active pocket of the enzyme. The same explanation holds true in case of next halogen-substituted compound **22 (**IC_{50} = 0.799 ± 0.008 μg/ml) in which fluoro group is present at *para*-position on the ring B. Afterwards, the next most potent derivative is compound **6** (IC_{50} = 0.284 ± 0.018 μg/ml) which contains strong electron-withdrawing group (–NO_2) at 4′ -position on ring B. Interestingly, the *meta* nitro substituted compound **9** (IC_{50} = 2.564 ± 0.0251 μg/ml) exhibited decreased activity as compared to its *para* analog **6**. The nitro group at *meta* position (ring B) might be creating steric hindrance, thus results in reduced activity.

Furthermore, the replacement of aryl ring B with other heterocyclic rings such as thiophene in compound **10** (IC_{50} = 0.347 ± 0.078 μg/ml) also displayed exceptional activity as compared to the standard (Table 4). The tyrosinase inhibition by compound **10** relied on the ability of a sulfur atom to coordinate with the dinuclear copper in the active site of the enzyme. Subsequently, the next synthetic analogue with comparable IC_{50} value is compound **11** (IC_{50} = 0.327 ± 0.041 μg/ml). This compound also showed stronger inhibitory activity against tyrosinase enzyme than the reference standard inhibitor Kojic acid. This might be a result of the strong chelation of electron-rich moiety (triphenylamine) of the derivative **11** with the active electrophilic centre of the tyrosinase. Finally, the analog **14** (IC_{50} = 0.370 ± 0.025 μg/ml), possessing bulky and polar sulphonamide-like group in the place of ring B, also showed outstanding activity against tyrosinase. The increased activity by **14** might be due to its position and effective interactions with the active pocket of the enzyme. Apart from that, all other synthetic 3-hydroxyflavones demonstrated good to moderate inhibitory activity against mushroom tyrosinase. Overall, the results presented herein show that the nature and pattern of substitution at both rings A and B enhance the inhibitory potential of these compounds, and thus are accountable to control it. Since all the proposed structures have a common 3-hydroxyflavone skeleton in their scaffolds.

Molecular modelling studies

In order to gain insight into the most probable binding conformation of 3-hydroxyflavone derivatives (**1-23**) with the active site of an enzyme and confirm the experimental results, the molecular docking studies were performed against mushroom tyrosinase enzyme. In this connection, 2-D structures of the compounds (**1-23**) were built up by using Chemdraw and then converted into 3-D by using Chem Pro3D software. The ligands were energetically minimized according to Merck Molecular Force Field (MMFF) and docked to the protein by using autodock1.5.6. By placements, the method will check 100 different poses into the active site pockets of 2Y9X and will result out of few best placements in the form of a histogram. For each conformer with the best (minimum) docking score was saved in preferences. Docking results are listed in Table 5. We have listed only the most excellent conformers and the docking score for each compound. The ligand developing most stable drug-receptor complex is the one which is having a minimum docking score. Validation of docking studies is evaluated by RMSD between the experimentally docking-observed and the x-ray ligand. The co-crystalline ligand was detached from the active pockets of the targeted substrate and the re-docked to calculate the RMSD value (Azam et al., 2012; Ounthaisong & Tangyuenyongwatana, 2017). The RMSD value of the re-docking of the co-crystalline ligand is 0.358 A^0, which depicts the validation of the docking process. The drug-receptor complexes of some potent ligands were analysed for various types of interactions such as hydrogen bonding, hydrophobic type interactions, and van der Waals interactions, etc.

The ligand (**5**) with binding energy (−8.55 Kcal mol^{-1}) articulated its inhibitory characteristics against the targeted biological specimen (2Y9X) via versatile kinds of associations. The ligand (**5**) coordinates with Ala286, Val283, and Val248 amino acid residues of the active site of tyrosinase through hydrophobic-π-alkyl type interaction. Delocalized π-electronic cloud of aromatic ring (A) of this ligand build up hydrophobic π- π stacked force of attraction with His263. Similarly, the alcoholic group (–OH) of the ring (C) engaged with the Glu256 by conventional hydrogen bonding. His259 also showed hydrogen bonding with the ligand **5** as shown in Figures 5 and 6.

Likewise, the ligand **14** could be an important inhibitor for the targeted biological receptor protein. Docking score

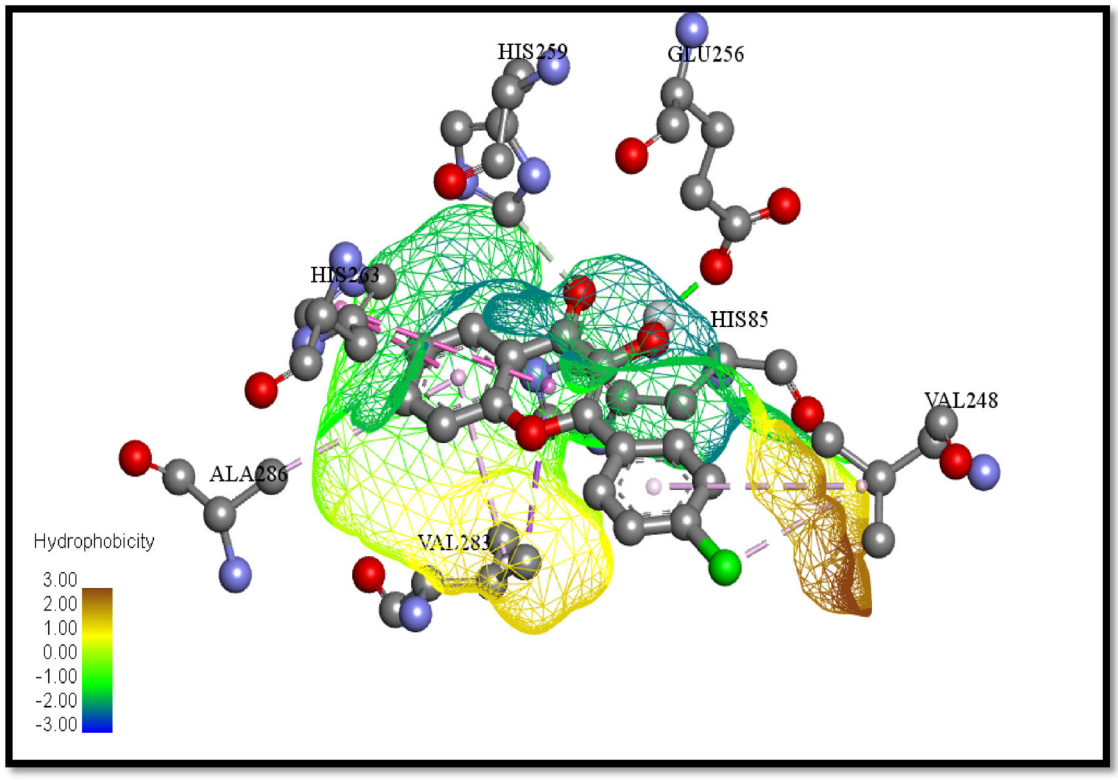

Figure 5. Putative binding associations of ligand **5** inside the active pockets of tyrosinase.

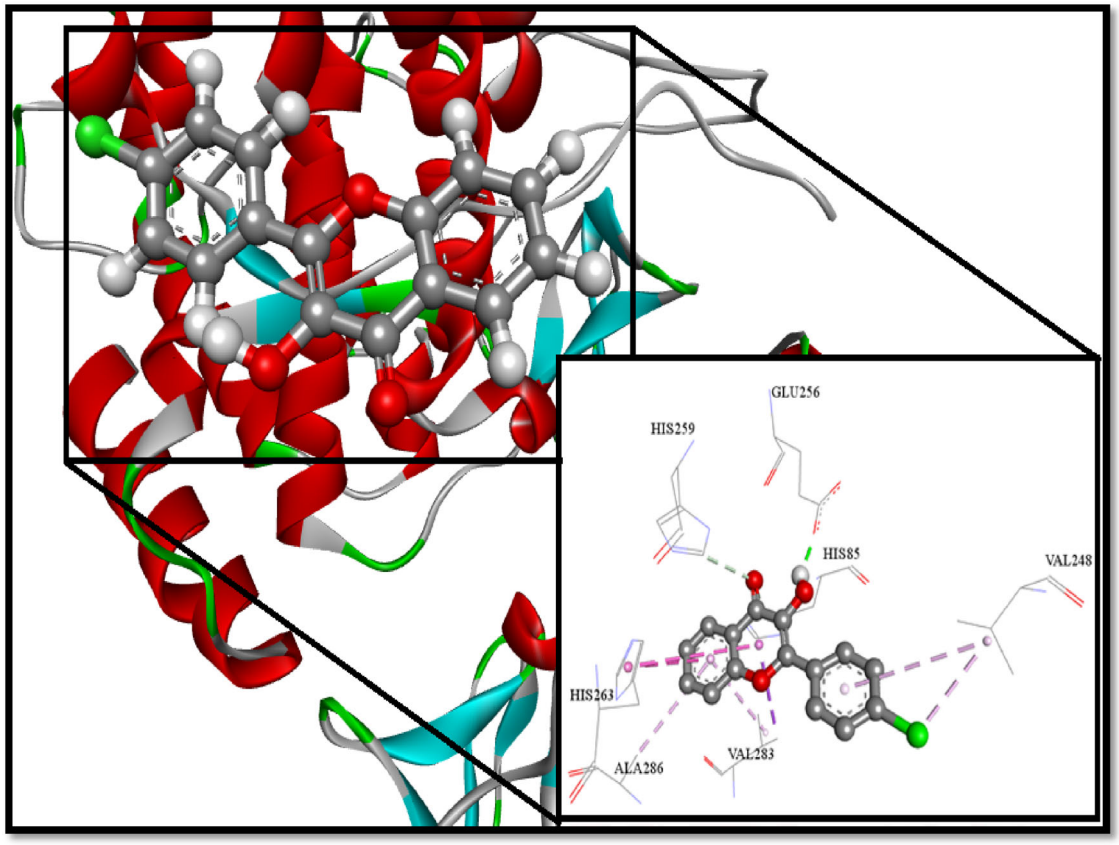

Figure 6. Associations of the ligand **5** against tyrosinase at 3D space. Box in the lower right corner shows the associations of specific amino acid residues. The 3D ribbon attributes the enzyme-stick model along with the lowest energy conforms of the inhibitor **5** and amino acids of tyrosinase interacting with it.

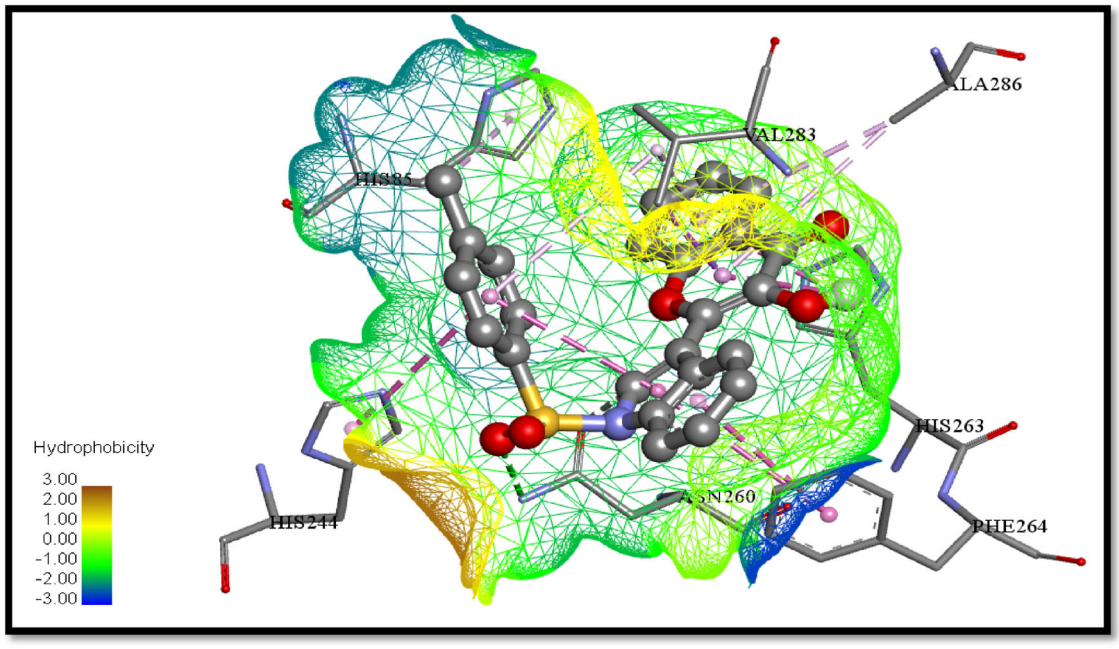

Figure 7. Putative binding associations of ligand **14** inside the active pockets of tyrosinase enzyme.

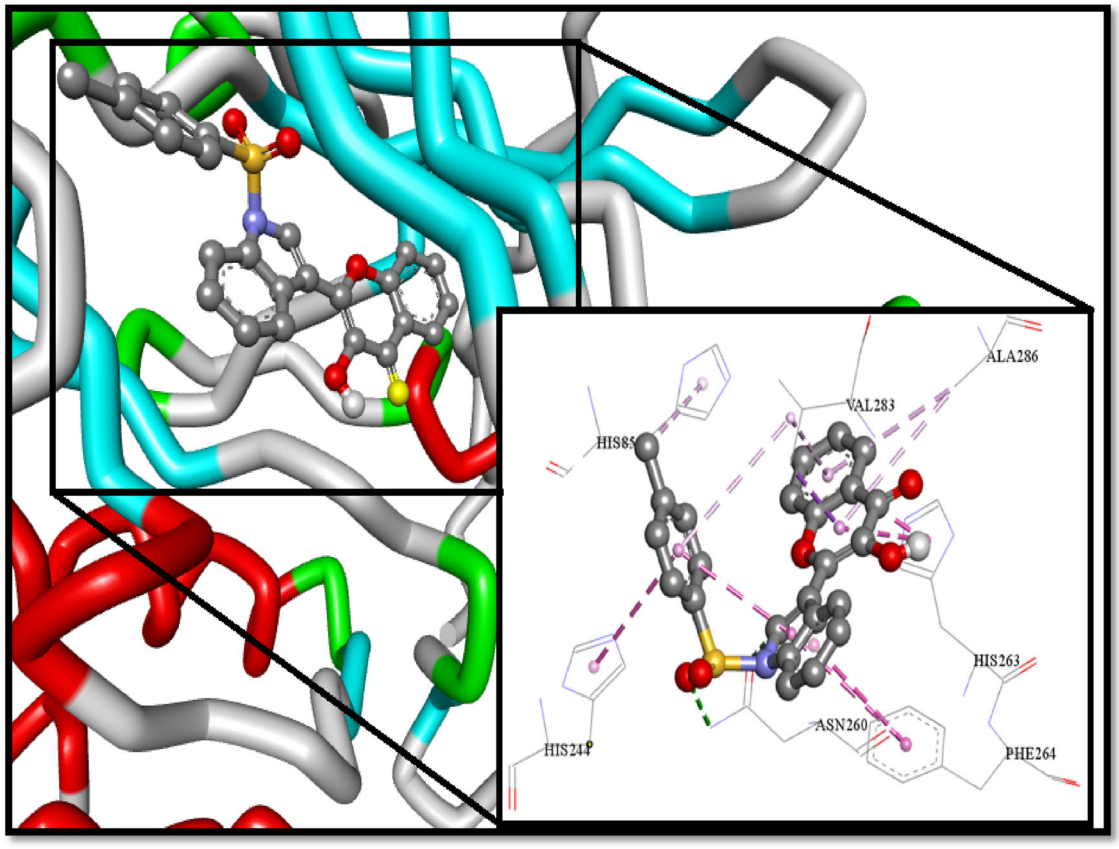

Figure 8. Associations of the ligand **14** against tyrosinase at 3D space. Box in the lower right corner shows the associations of specific amino acid residues. The 3D ribbon attributes the enzyme-stick model along with the lowest energy conforms of the inhibitor **14** and amino acids of tyrosinase interacting with it.

(−8.59 Kcal mol^{-1}) of the ligand **14** is due to some important type of linkages such as it exhibits hydrogen bonding with Asn260 amino acid residues inside the active pockets of the protein 2Y9X. This ligand expressed its inhibitory potential by possessing hydrophobic π-alkyl, hydrophobic π-σ, hydrophobic π-π T-shaped and hydrophobic π-π Stacked type interactions with His263, Phe264, Ala286, Val283, and His85 amino acid residues inside of activation loop of targeted tyrosinase biological molecule as displayed in Figures 7 and 8.

Conclusions

In summary, we have efficiently synthesized a series of 3-hydroxyflavone derivatives (1-23) containing different functional groups using precedented Algar-Flynn-Oyamada reaction in a one-pot synthesis. These synthetic compounds were then evaluated *in vitro* for their inhibitory activity against mushroom tyrosinase enzyme. Among the series, derivatives (**2, 4, 5, 6, 7, 10, 11, 14,** and **22**) exhibited the most potent inhibitory influence on mushroom tyrosinase, even better than the standard. Notably, the compound **5** displayed maximum inhibition against tyrosinase with (IC_{50} = 0.230 ± 0.020 μg/ml) demonstrating that **5** was about sevenfold more effective mushroom tyrosinase inhibitor as compared to Kojic acid (IC_{50} =1.79 ± 0.6 μg/ml). Limited SAR studies showed that all structural features were contributing to tyrosinase inhibition, however, flavonols with functional groups such as F, Cl, NO_2, CF_3, triphenylamine, and sulphonamide moieties present at *meta*- and *para*-positions on ring B were actively taking part in the activity. Additionally, the antimicrobial assay of the synthetic derivatives (**1-23**) showed good to moderate activities, however, none of the compounds was active more than the standard Cefixime and Clotrimazole. Moreover, the emission behavior of these synthetic flavonols was also investigated. Results showed that they emit light at longer wavelengths upon excitation around 330 nm wavelength. To recognize the structural features that were involved in the binding interactions with the active site of tyrosinase, *in silico* study was also performed. The above-mentioned results suggest that these molecules can serve as fascinating candidates for the treatment of tyrosinase-related ailments and as lead compounds for the development of potent new tyrosinase inhibitors and antimicrobial agents. Hence, more results aiming at the investigation of these potent compounds against test enzyme and their mechanistic studies are underway in our group and will be reported in due course in the future.

Acknowledgements

We are grateful to Prof. Dr. Norbert Sewald, Department of Organic Chemistry III, Bielefeld University, Germany and Dr. Renhao Dong, Department of Chemistry, Dresden University, Germany for their help in spectroscopic measurements.

Disclosure statement

No potential conflict of interest was reported by the author(s).

Funding

This research work was financially supported by the Higher Education Commission of Pakistan under the NRPU Project No. 6484. M.M. acknowledges financial support from Ferdowsi University of Mashhad. M.M. is also supported by the Iran Science Elites Federation and Zeolite and Porous Materials Committee of Iranian Chemical Society.

References

Agullo, G., Gamet-Payrastre, L., Manenti, S., Viala, C., Rémésy, C., Chap, H., & Payrastre, B. (1997). Relationship between flavonoid structure and inhibition of phosphatidylinositol 3-kinase: A comparison with tyrosine kinase and protein kinase C inhibition. *Biochemical Pharmacology*, *53*(11), 1649–1657. https://doi.org/10.1016/s0006-2952(97)82453-7

Aherne, S. A., & O'Brien, N. M. (2002). Dietary flavonols: Chemistry, food content, and metabolism. *Nutrition (Burbank, Los Angeles County, Calif.)*, *18*(1), 75–81. https://doi.org/10.1016/s0899-9007(01)00695-5

Akiyama, T., Ishida, J., Nakagawa, S., Ogawara, H., Watanabe, S-i., Itoh, N., Shibuya, M., & Fukami, Y. (1987). Genistein, a specific inhibitor of tyrosine-specific protein kinases. *The Journal of Biological Chemistry*, *262*(12), 5592–5595.

Ali, A., Ashraf, Z., Kumar, N., Rafiq, M., Jabeen, F., Park, J. H., Choi, K. H., Lee, S., Seo, S.-Y., Choi, E. H., & Attri, P. (2016). Influence of plasma-activated compounds on melanogenesis and tyrosinase activity. *Scientific Reports*, *6*(1), 1–20. https://doi.org/10.1038/srep21779

Alluis, B., Pérol, N., El Hajji, H., & Dangles, O. (2000). Water-soluble flavonol (= 3-Hydroxy-2-phenyl-4H-1-benzopyran-4-one) derivatives: Chemical synthesis, colouring, and antioxidant properties. *Helvetica Chimica Acta*, *83*(2), 428–443. https://doi.org/10.1002/(SICI)1522-2675(20000216)83:2<428::AID-HLCA428>3.0.CO;2-J

Altaf, A. A., Khan, N., Lal, B., & Badshah, A. (2017). Synthesis, characterization and DNA-intercalation studies of two ferrocene-based Fe-Sn heterobimetallic compounds, and crystal structure of trimethyltin (p-ferrocenyl) benzoate. *Journal of Coordination Chemistry*, *70*(20), 3523–3540. https://doi.org/10.1080/00958972.2017.1384547

Azam, S. S., Uddin, R., & Syed, A. A. S. (2012). Molecular docking studies of potent inhibitors of tyrosinase and α-glucosidase. *Medicinal Chemistry Research*, *21*(8), 1677–1683.

Bansal, M., & Kaur, R. (2015). Electromeric effect of substitution at 6 th position in 2-(Furan-2-yl)-3-hydroxy-4 H-chromen-4-one (FHC) on the absorption and emission spectra. *Journal of Chemical Sciences*, *127*(3), 405–412. https://doi.org/10.1007/s12039-015-0786-1

Benavente-García, O., Castillo, J., Marin, F. R., Ortuño, A., & Del Río, J. A. (1997). Uses and properties of citrus flavonoids. *Journal of Agricultural and Food Chemistry*, *45*(12), 4505–4515. https://doi.org/10.1021/jf970373s

Bruker, M. (2016). *APEX3 and SADABS*. Bruker AXS Inc.

Chang, T.-S. (2009). An updated review of tyrosinase inhibitors. *International Journal of Molecular Sciences*, *10*(6), 2440–2475. https://doi.org/10.3390/ijms10062440

Chen, Q.-X., & Kubo, I. (2002). Kinetics of mushroom tyrosinase inhibition by quercetin. *Journal of Agricultural and Food Chemistry*, *50*(14), 4108–4112. https://doi.org/10.1021/jf011378z

Cody, V., Middleton, E., Harborne, J. B. (1986). Plant flavonoids in biology and medicine: Biochemical, pharmacological, and structure-activity relationships. *Proceedings of a Symposium Held in Buffalo* (pp. 22–26).

Cooksey, C. J., Garratt, P. J., Land, E. J., Pavel, S., Ramsden, C. A., Riley, P. A., & Smit, N. P. (1997). Evidence of the indirect formation of the catecholic intermediate substrate responsible for the autoactivation kinetics of tyrosinase. *The Journal of Biological Chemistry*, *272*(42), 26226–26235. https://doi.org/10.1074/jbc.272.42.26226

Cushman, M., Nagarathnam, D., & Geahlen, R. L. (1991). Synthesis and evaluation of hydroxylated flavones and related compounds as potential inhibitors of the protein-tyrosine kinase p56lck. *Journal of Natural Products*, *54*(5), 1345–1352. https://doi.org/10.1021/np50077a018

Ehsan, S., Faisal, S., & Akbar, W. (2016). A facile microwave-assisted synthesis of 3-hydroxy-2-phenyl-4h-chromen-4-one and its derivatives via a novel approach. *Journal of the Chemical Society of Pakistan*, *38*(6), 1190–1195.

Fairhead, M., & Thöny-Meyer, L. (2012). Bacterial tyrosinases: Old enzymes with new relevance to biotechnology. *New Biotechnology*, *29*(2), 183–191. https://doi.org/10.1016/j.nbt.2011.05.007

Farhadi, F., Khameneh, B., Iranshahi, M., & Iranshahy, M. (2019). Antibacterial activity of flavonoids and their structure–activity relationship: An update review. *Phytotherapy Research: PTR*, *33*(1), 13–40. https://doi.org/10.1002/ptr.6208

Ferriola, P. C., Cody, V., & Middleton, E. (1989). Protein kinase C inhibition by plant flavonoids: Kinetic mechanisms and structure-activity relationships. *Biochemical Pharmacology*, *38*(10), 1617–1624. https://doi.org/10.1016/0006-2952(89)90309-2

Gamet-Payrastre, L., Manenti, S., Gratacap, M.-P., Tulliez, J., Chap, H., & Payrastre, B. (1999). Flavonoids and the inhibition of PKC and PI 3-kinase. *General Pharmacology*, *32*(3), 279–286. https://doi.org/10.1016/S0306-3623(98)00220-1

García-Lafuente, A., Guillamón, E., Villares, A., Rostagno, M. A., & Martínez, J. A. (2009). Flavonoids as anti-inflammatory agents: Implications in cancer and cardiovascular disease. *Inflammation Research: Official Journal of the European Histamine Research Society*, *58*(9), 537–552. https://doi.org/10.1007/s00011-009-0037-3

Garcia-Rivera, J., & Casadevall, A. (2001). Melanization of *Cryptococcus neoformans* reduces its susceptibility to the antimicrobial effects of silver nitrate. *Medical Mycology*, *39*(4), 353–357. https://doi.org/10.1080/714031043

Geng, J., Yu, S.-B., Wan, X., Wang, X.-J., Shen, P., Zhou, P., & Chen, X.-D. (2008). Protective action of bacterial melanin against DNA damage in full UV spectrums by a sensitive plasmid-based noncellular system. *Journal of Biochemical and Biophysical Methods*, *70*(6), 1151–1155. https://doi.org/10.1016/j.jprot.2007.12.013

Golub, A. G., Bdzhola, V. G., Kyshenia, Y. V., Sapelkin, V. M., Prykhod'ko, A. O., Kukharenko, O. P., Ostrynska, O. V., & Yarmoluk, S. M. (2011). Structure-based discovery of novel flavonol inhibitors of human protein kinase CK2. *Molecular and Cellular Biochemistry*, *356*(1–2), 107–115. https://doi.org/10.1007/s11010-011-0945-8

Gunduz, S., Goren, A. C., & Ozturk, T. (2012). Facile syntheses of 3-hydroxyflavones. *Organic Letters*, *14*(6), 1576–1579. https://doi.org/10.1021/ol300310e

Gupta, S., Kumar, N., Kumar, S., Dudhe, R., & Sharma, P. (2012). 3-Hydroxy-2-(substituted phenyl)-4H-chromen-4-one derivatives-synthesis, spectral characterization and pharmacological screening. *International Journal of Toxicology*, *7*, 1–8.

Gupta, V. K., Mergu, N., & Singh, A. K. (2014). Fluorescent chemosensors for Zn^{2+} ions based on flavonol derivatives. *Sensors and Actuators B: Chemical*, *202*, 674–682. https://doi.org/10.1016/j.snb.2014.05.133

Haslam, E. (1998). *Practical polyphenolics: From structure to molecular recognition and physiological action*. Cambridge University Press.

Hearing, V. J., & Jiménez, M. (1989). Analysis of mammalian pigmentation at the molecular level. *Pigment Cell Research*, *2*(2), 75–85. https://doi.org/10.1111/j.1600-0749.1989.tb00166.x

Höfener, S., Kooijman, P. C., Groen, J., Ariese, F., & Visscher, L. (2013). Fluorescence behavior of (selected) flavonols: A combined experimental and computational study. *Physical Chemistry Chemical Physics: PCCP*, *15*(30), 12572–12581. https://doi.org/10.1039/c3cp44267e

Hollman, P. C. H., & Katan, M. B. (1999). Dietary flavonoids: Intake, health effects and bioavailability. *Food and Chemical Toxicology: An International Journal Published for the British Industrial Biological Research Association*, *37*(9–10), 937–942. https://doi.org/10.1016/S0278-6915(99)00079-4

Hussin, N., Muse, R., Ahmad, S., Ramli, J., Mahmood, M., Sulaiman, M., Shukor, M., Rahman, M., & Aziz, K. (2009). Antifungal activity of extracts and phenolic compounds from *Barringtonia racemosa* L.(Lecythidaceae). *African Journal of Biotechnology*, *8*(12), 2835–2842.

Kaur, R., Kaur, K., & Bansal, M. (2017). Comparative studies in the fluorescence and excitation spectra of 3-hydroxyflavone and 2 (2'-heteroaryl)-3-hydroxy-4H-chromen-4-ones. *Journal of Applied Spectroscopy*, *84*(2), 242–248. https://doi.org/10.1007/s10812-017-0458-7

Khanna, R., Kumar, R., Dalal, A., & Kamboj, R. C. (2015). Absorption and fluorescent studies of 3-hydroxychromones. *Journal of Fluorescence*, *25*(5), 1159–1163. https://doi.org/10.1007/s10895-015-1623-0

Kim, D., Park, J., Kim, J., Han, C., Yoon, J., Kim, N., Seo, J., & Lee, C. (2006). Flavonoids as mushroom tyrosinase inhibitors: A fluorescence quenching study. *Journal of Agricultural and Food Chemistry*, *54*(3), 935–941. https://doi.org/10.1021/jf0521855

Klymchenko, A. S., Ozturk, T., Pivovarenko, V. G., & Demchenko, A. P. (2001). A 3-hydroxychromone with dramatically improved fluorescence properties. *Tetrahedron Letters*, *42*(45), 7967–7970. https://doi.org/10.1016/S0040-4039(01)01723-3

Kumar, S., & Pandey, A. K. (2013). Chemistry and biological activities of flavonoids: An overview. *The Scientific World Journal*, *2013*, 1–16. https://doi.org/10.1155/2013/162750

Lal, B., Akhter, S., Altaf, A. A., Badshah, A., Hussain, R. A., & Li, H. (2016). Synthesis, crystal structure, spectral and electrochemical characterization, DNA binding and antioxidant studies of 1-(2-florobenzoyl)-3-(2-chloro, 4-ferrocenylphenyl) thiourea. *Inernational Journal of Electrochemical Science*, *11*, 1632–1639.

Linassier, C., Pierre, M., Le Pecq, J.-B., & Pierre, J. (1990). Mechanisms of action in NIH-3T3 cells of genistein, an inhibitor of EGF receptor tyrosine kinase activity. *Biochemical Pharmacology*, *39*(1), 187–193. https://doi.org/10.1016/0006-2952(90)90664-7

Liu, S., Li, D., Huang, B., Chen, Y., Lu, X., & Wang, Y. (2013). Inhibition of pancreatic lipase, α-glucosidase, α-amylase, and hypolipidemic effects of the total flavonoids from *Nelumbo nucifera* leaves. *Journal of Ethnopharmacology*, *149*(1), 263–269. https://doi.org/10.1016/j.jep.2013.06.034

Lopez-Lazaro, M. (2002). Flavonoids as anticancer agents: Structure-activity relationship study. *Current Medicinal Chemistry-Anti-Cancer Agents*, *2*(6), 691–714.

Macrae, C. F., Edgington, P. R., McCabe, P., Pidcock, E., Shields, G. P., Taylor, R., Towler, M., & Streek, J. (2006). Mercury: Visualization and analysis of crystal structures. *Journal of Applied Crystallography*, *39*(3), 453–457. https://doi.org/10.1107/S002188980600731X

Maeda, K., & Fukuda, M. (1996). Arbutin: Mechanism of its depigmenting action in human melanocyte culture. *The Journal of Pharmacology and Experimental Therapeutics*, *276*(2), 765–769.

Maeda, K., & Yoshizaki, K. (1991). Interstitial term pregnancy without rupture. *Nihon Sanka Fujinka Gakkai Zasshi*, *43*(3), 361–363.

Manthey, J. A., Guthrie, N., & Grohmann, K. (2001). Biological properties of citrus flavonoids pertaining to cancer and inflammation. *Current Medicinal Chemistry*, *8*(2), 135–153. https://doi.org/10.2174/0929867013373723

Middleton, E. (1996). Biological properties of plant flavonoids: An overview. *International Journal of Pharmacognosy*, *34*(5), 344–348.

Mughal, E. U., Javid, A., Sadiq, A., Murtaza, S., Zafar, M. N., Khan, B. A., Sumrra, S. H., Tahir, M. N., & Khan, K. M. (2018). Synthesis, structure-activity relationship and molecular docking studies of 3-*O*-flavonol glycosides as cholinesterase inhibitors. *Bioorganic & Medicinal Chemistry*, *26*(12), 3696–3706.

Mughal, E. U., Sadiq, A., Ashraf, J., Zafar, M. N., Sumrra, S. H., Tariq, R., Mumtaz, A., Javid, A., Khan, B. A., Ali, A., & Javed, C. O. (2019). Flavonols and 4-thioflavonols as potential acetylcholinesterase and butyrylcholinesterase inhibitors: Synthesis, structure-activity relationship and molecular docking studies. *Bioorganic Chemistry*, *91*, 103124. https://doi.org/10.1016/j.bioorg.2019.103124

Mughal, E. U., Sadiq, A., Hamayun, M., Zafar, M. N., Fatima, N., Yameen, M. A., Muhammad, S. A., Mumtaz, A., Ahmed, I., & Fatima, T. (2018). Design, synthesis and biological evaluation of novel dihydropyrimidine-2-thione derivatives as potent antimicrobial agents: Experimental and molecular docking approach. *Letters in Drug Design & Discovery*, *15*(11), 1189–1201. https://doi.org/10.2174/1570180815666180209151516

Nhu, D., Hawkins, B. C., & Burns, C. J. (2015). Phase transfer catalysis extends the scope of the Algar–Flynn–Oyamada synthesis of 3-hydroxyflavones. *Australian Journal of Chemistry*, *68*(7), 1102–1107. https://doi.org/10.1071/CH14620

Nihei, K-i., & Kubo, I. (2003). Identification of oxidation product of arbutin in mushroom tyrosinase assay system. *Bioorganic & Medicinal Chemistry Letters*, *13*(14), 2409–2412. https://doi.org/10.1016/S0960-894X(03)00395-0

Nosanchuk, J. D., & Casadevall, A. (2003). The contribution of melanin to microbial pathogenesis. *Cellular Microbiology*, *5*(4), 203–223. https://doi.org/10.1046/j.1462-5814.2003.00268.x

Ounthaisong, U., & Tangyuenyongwatana, P. (2017). Cross docking study of flavanoids against tyrosinase enzymes using PyRx 0.8 virtual screening tool. *Thai Journal of Pharmaceutical Sciences*, *41*(17), 189–192.

Promden, W., Viriyabancha, W., Monthakantirat, O., Umehara, K., Noguchi, H., & De-Eknamkul, W. (2018). Correlation between the potency of flavonoids on mushroom tyrosinase inhibitory activity and

melanin synthesis in melanocytes. Molecules, *23*(6), 1403. https://doi.org/10.3390/molecules23061403

Qin, H.-L., Shang, Z.-P., Jantan, I., Tan, O. U., Hussain, M. A., Sher, M., & Bukhari, S. N. A. (2015). Molecular docking studies and biological evaluation of chalcone based pyrazolines as tyrosinase inhibitors and potential anticancer agents. *RSC Advances*, *5*(57), 46330–46338. https://doi.org/10.1039/C5RA02995C

Rao, K., Chodisetti, B., Gandi, S., Giri, A., & Kishor, P. K. (2016). Regeneration-based quantification of coumarins (Scopoletin and Scoparone) in *Abutilon indicum in vitro* cultures. *Applied Biochemistry and Biotechnology*, *180*(4), 766–779. https://doi.org/10.1007/s12010-016-2131-7

Ren, W., Qiao, Z., Wang, H., Zhu, L., & Zhang, L. (2003). Flavonoids: Promising anticancer agents. *Medicinal Research Reviews*, *23*(4), 519–534. https://doi.org/10.1002/med.10033

Rice-Evans, C. A., Miller, N. J., Bolwell, P. G., Bramley, P. M., & Pridham, J. B. (1995). The relative antioxidant activities of plant-derived polyphenolic flavonoids. *Free Radical Research*, *22*(4), 375–383. https://doi.org/10.3109/10715769509145649

Saleem, L., Altaf, A. A., Badshah, A., Rauf, M. K., Waseem, A., Danish, M., Azam, S. S., Arshad, M. N., Asiri, A. M., Ahmad, S., & Gul, R. (2018). Structural investigations, anti-leishmanial, antibacterial and docking studies of new pentavalent antimony carboxylates. *Inorganica Chimica Acta*, *474*, 148–155. https://doi.org/10.1016/j.ica.2018.01.036

Seleem, D., Pardi, V., & Murata, R. M. (2017). Review of flavonoids: A diverse group of natural compounds with anti-*Candida albicans* activity in vitro. *Archives of Oral Biology*, *76*, 76–83. https://doi.org/10.1016/j.archoralbio.2016.08.030

Seo, W. D., Ryu, Y. B., Curtis-Long, M. J., Lee, C. W., Ryu, H. W., Jang, K. C., & Park, K. H. (2010). Evaluation of anti-pigmentary effect of synthetic sulfonylamino chalcone. *European Journal of Medicinal Chemistry*, *45*(5), 2010–2017. https://doi.org/10.1016/j.ejmech.2010.01.049

Singh, A. K., Saxena, G., & Arshad, M. (2017). Synthesis, characterization and biological evaluation of ruthenium flavanol complexes against breast cancer. *Spectrochimica Acta Part A: Molecular and Biomolecular Spectroscopy*, *180*, 97–104. https://doi.org/10.1016/j.saa.2017.02.056

Şöhretoğlu, D., Sari, S., Barut, B., & Özel, A. (2018). Tyrosinase inhibition by some flavonoids: Inhibitory activity, mechanism by *in vitro* and *in silico* studies. *Bioorganic Chemistry*, *81*, 168–174. https://doi.org/10.1016/j.bioorg.2018.08.020

Spek, A. L. (2009). Structure validation in chemical crystallography. *Acta Crystallographica. Section D, Biological Crystallography*, *65*(Pt 2), 148–155. https://doi.org/10.1107/S090744490804362X

Spek, A. L. (2015). PLATON SQUEEZE: A tool for the calculation of the disordered solvent contribution to the calculated structure factors. *Acta Crystallographica Section C Structural Chemistry*, *71*(1), 9–18. https://doi.org/10.1107/S2053229614024929

Strack, D., Wray, V., & Harborne, J. (1994). *The flavonoids: Advances in research since 1986*. Chapman and Hall.

Tsao, R. (2010). Chemistry and biochemistry of dietary polyphenols. Nutrients, *2*(12), 1231–1246. https://doi.org/10.3390/nu2121231

Tschesche, R., Delhvi, S., Sepulveda, S., & Breitmaier, E. (1979). Eucryphin, a new chromone rhamnoside from the bark of *Eucryphia cordifolia*. Phytochemistry, *18*(5), 867–869. https://doi.org/10.1016/0031-9422(79)80032-1

Tsuji-Naito, K., Hatani, T., Okada, T., & Tehara, T. (2007). Modulating effects of a novel skin-lightening agent, alpha-lipoic acid derivative, on melanin production by the formation of DOPA conjugate products . *Bioorganic & Medicinal Chemistry*, *15*(5), 1967–1975. https://doi.org/10.1016/j.bmc.2006.12.042

Verma, A. K., & Pratap, R. (2010). The biological potential of flavones. *Natural Product Reports*, *27*(11), 1571–1593. https://doi.org/10.1039/c004698c

Walle, T., Walgren, R., Walle, U., Galijatovic, A., & Vaidyanathan, J. (2003). *Flavonoids in health and disease*. In C. A. Rice-Evans & L. Packer (Eds.). CRC Press.

Xia, L., Idhayadhulla, A., Lee, Y. R., Kim, S. H., & Wee, Y.-J. (2014). Antioxidant and antibacterial evaluation of synthetic furomollugin and its diverse analogs. *Medicinal Chemistry Research*, *23*(7), 3528–3538. https://doi.org/10.1007/s00044-014-0929-9

Yoshida, K., Mori, M., & Kondo, T. (2009). Blue flower color development by anthocyanins: From chemical structure to cell physiology. *Natural Product Reports*, *26*(7), 884–915. https://doi.org/10.1039/b800165k

You, J., Fu, H., Zhao, D., Hu, T., Nie, J., & Wang, T. (2020). Flavonol dyes with different substituents in photopolymerization. *Journal of Photochemistry and Photobiology A: Chemistry*, *386*, 112097. https://doi.org/10.1016/j.jphotochem.2019.112097

Yuan, Y., Jin, W., Nazir, Y., Fercher, C., Blaskovich, M. A., Cooper, M. A., Barnard, R. T., & Ziora, Z. M. (2020). Tyrosinase inhibitors as potential antibacterial agents. *European Journal of Medicinal Chemistry*, *187*, 111892. https://doi.org/10.1016/j.ejmech.2019.111892

Zolghadri, S., Bahrami, A., Hassan Khan, M. T., Munoz-Munoz, J., Garcia-Molina, F., Garcia-Canovas, F., & Saboury, A. A. (2019). A comprehensive review on tyrosinase inhibitors. *Journal of Enzyme Inhibition and Medicinal Chemistry*, *34*(1), 279–309. https://doi.org/10.1080/14756366.2018.1545767